Article

Sila-Ibuprofen

Florian Kleemiss, Aileen Justies, Daniel Duvinage, Patrick Watermann, Eric Ehrke, Kunihisa Sugimoto, Malte Fugel, Lorraine A. Malaspina, Anneke Dittmer, Torsten Kleemiss, Pim Puylaert, Nelly R. King, Anne Staubitz, Thomas M. Tzschentke, Ralf Dringen, Simon Grabowsky, and Jens Beckmann

J. Med. Chem., **Just Accepted Manuscript** • DOI: 10.1021/acs.jmedchem.0c00813 • Publication Date (Web): 15 Sep 2020

Sila-Ibuprofen

Florian Kleemiss[1,2], Aileen Justies[3], Daniel Duvinage[2], Patrick Watermann[4], Eric Ehrke[4], Kunihisa Sugimoto[5,6], Malte Fugel[1], Lorraine A. Malaspina[1], Anneke Dittmer[1], Torsten Kleemiss[1], Pim Puylaert[1], Nelly R. King[3], Anne Staubitz[7], Thomas M. Tzschentke[8], Ralf Dringen[4], Simon Grabowsky[1,2*], Jens Beckmann[1,3*]

[1] University of Bremen, Institute for Inorganic Chemistry and Crystallography, Leobener Str. 3 and 7, 28359 Bremen, Germany. [2] University of Bern, Department of Chemistry and Biochemistry, Freiestrasse 3, 3012 Bern, Switzerland. [3] Free University of Berlin, Institute of Chemistry and Biochemistry, Fabeckstr. 34-36, 14195 Berlin, Germany. [4] University of Bremen, Center for Biomolecular Interactions Bremen and Center for Environmental Research and Sustainable Technology, Leobener Str. 5, 28359 Bremen, Germany. [5] Japan Synchrotron Radiation Research Institute (JASRI), Diffraction & Scattering Division, 1-1-1 Kouto, Sayo-cho, Sayo-gun, Hyogo 679-5198, Japan. [6] Institute for Integrated Cell-Material Sciences (iCeMS), Kyoto University, Yoshida-Ushinomiya-cho, Sakyo-ku, Kyoto 606-8501, Japan. [7] University of Bremen, Institute for Analytical and Organic Chemistry, Leobener Str. 7, 28359 Bremen, Germany. [8] Grünenthal GmbH, Steinfeldstr. 2, 52222 Stolberg, Germany.

ABSTRACT The synthesis, characterization, biological activity and toxicology of sila-ibuprofen, a silicon derivative of the most common non-steroidal anti-inflammatory drug, is reported. Key improvements compared to ibuprofen are a four times higher solubility in physiological media and a lower melting enthalpy, which were attributed to the carbon-silicon switch. The improved solubility is of interest for post-surgical intravenous administration. A potential for pain relief is rationalized via inhibition experiments of cyclooxygenases I and II (COX-I and COX-II) as well as via a set of newly developed methods that combine molecular dynamics, quantum chemistry and quantum crystallography. The binding affinity of sila-ibuprofen to COX-I and COX-II is quantified in terms of London dispersion and electrostatic interactions in the active receptor site. This study shows not only the potential of sila-ibuprofen for medicinal application, but also improves our understanding of the mechanism of action of the inhibition process.

INTRODUCTION

Ibuprofen (**1**), a non-steroidal anti-inflammatory drug, is the gold-standard in pain relief medication. It is listed in the "essential medicines list" of the World Health Organization.[1] The mechanism of action involves the inhibition of cyclooxygenase-II (COX-II), thus blocking the synthesis of prostaglandins from arachidonic acid.[2] In contrast to COX-I, which is permanently present in the body, COX-II is only produced when actual damage to the tissue or inflammation occurs. It is expressed in macrophages and synthesizes prostaglandins responsible for initial inflammation and body temperature increase. It is also expressed by endothelial cells of proliferating blood vessels and, in case of inflammation, by endothelial cells of the hypothalamus.[3]

In this work, we show that ibuprofen, the gold-standard in non-steroidal anti-rheumatic treatments, can still be fine-tuned and improved by the formal exchange of a carbon against a silicon atom (carbon-silicon switch).[4] We describe the synthesis of sila-ibuprofen (**2**), its full characterization as well as toxicological and *in-vitro* investigations on its pharmacological potency. The observed properties are explained using a newly developed approach based on method development in molecular dynamics (MD), quantum crystallography and quantum-chemical characterization of non-covalent interactions that allows to quantify differences and similarities between **1** and **2**.

RESULTS AND DISCUSSION

The synthesis of sila-ibuprofen (**2**) was achieved in a one-pot reaction starting from commercially available 2-[(4-bromomethyl) phenyl] propionic acid and dimethylchlorosilane, Me_2SiClH (Scheme 1).

Scheme 1. Lewis formulae of ibuprofen (**1**) and sila-ibuprofen (**2**), and synthesis of **2**.

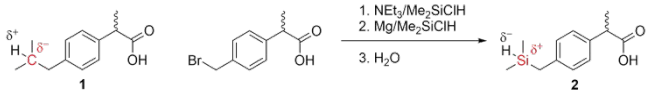

Me_2SiClH fulfils two functions. In combination with triethylamine, NEt_3, it introduces a silyl ester that protects the carboxylic acid group prior to a Barbier-reaction of the bromomethyl group with magnesium and Me_2SiClH. A subsequent aqueous work-up deprotects the carboxylic acid and affords **2** after purification by column chromatography as a microcrystalline colorless solid in 85 % yield. The ^{1}H and $^{13}C\{^{1}H\}$ NMR spectra (acetone-d_6) of **2** show the expected number of signals and confirm purity. The $^{29}Si\{^{1}H\}$ NMR spectrum (acetone-d_6) of **2** shows a signal at δ = - 11.5 ppm with an indicative ^{1}J(Si-H) coupling constant of 185 Hz. The IR spectrum exhibits a characteristic signal at $\tilde{\nu}$ = 2132 cm^{-1}, which was assigned to a Si-H stretching vibration. Sila-ibuprofen (**2**) was obtained as a racemic mixture, which was used without optical resolution in this study. Although it is known that only the S-enantiomer of ibuprofen is biologically active, racemic mixtures are administered in medicinal treatments because an isomerase converts the enantiomers *in-vivo*.[3]

An important issue involving the application of ibuprofen is the low solubility in physiological media, which limits the use

in post-surgical intravenous treatments, and is related to the rather high melting point and high melting enthalpy (Table 1). The melting point of sila-ibuprofen (**2**, 45-47.5°C) is significantly lower than that of ibuprofen (**1**, 74-77°C), even lower than that of enantiomerically pure ibuprofen (54°C).[5] The melting enthalpy of **2** is 15.8 ± 0.5 kJ mol^{-1}, being lower than that of **1** (26.7 kJ mol^{-1}).[6] The solubility of **2** is 83 ± 3 mg L^{-1} in water, which is approximately four times higher than that of **1**, being 21 mg L^{-1} (Figure S1).[7] A NMR investigation of **2** under physiological conditions (pH 8, 40°C) suggests stability over a timespan of several weeks (Figures S5 – S6).

Measurements of the IC_{50} values of inhibition of human COX-I and II by **1** or **2** in buffered saline reveal the concentrations at which 50% of the enzymatic activity is inhibited (Table 1, Figure S29). Hence, both ibuprofen (**1**) and sila-ibuprofen (**2**) more selectively inhibit COX-II than COX-I, whereas the absolute values between **1** and **2** are similar for both enzymes.

Table 1. Key properties of ibuprofen (**1**) and sila-ibuprofen (**2**).

Property	Ibuprofen (**1**)	Sila-ibuprofen (**2**)
Melting Point /°C	74-77[5]	45-47.5
Melting Enthalpy /kJ mol^{-1}	26.7[6]	15.8 ± 0.5
Solubility (water) /mg L^{-1}	21	83 ± 3
IC_{50} (COX-I) /μM	34	26
IC_{50} (COX-II) /μM	3.3	8.3

A detailed discussion of how different assay conditions and parameters may affect absolute inhibition constants and relative COX-selectivity for nonsteroidal anti-inflammatory drugs is beyond the scope of the present paper and has been dis cussed in detail elsewhere.[8] Hence, within the expected uncertainty of such measurements, the silicon-carbon switch has affected the inhibition properties only slightly. In summary, all properties of sila-ibuprofen (**2**) suggest improved application in physiological media, while retaining a similar level of potency and mode of action compared to **1** (Table 1).

The most important metabolite of ibuprofen (**1**) is hydroxy-ibuprofen, which is formed upon enzymatic oxidation of the isobutyl (CH_2Me_2***C***-H) group.[3] It is an interesting scientific question, whether the dimethylsilylmethyl (CH_2Me_2***Si***-H) group will be oxidized similarly in an enzymatic reaction. Recent work by Arnold et al. suggests that enzymes are capable of activating the artificial Si–H bond and transforming it into Si–C bonds.[9] For sila-ibuprofen (**2**), this question remains unanswered for now, but the *in situ* chemical synthesis of the potential metabolite hydroxy-sila-ibuprofen was developed and described in the supporting material. Like many other silanols, hydroxy-sila-ibuprofen undergoes condensation to the related siloxane at higher concentrations.

The most significant changes relevant for the biochemical recognition of a molecule introduced by a carbon-silicon switch include bond lengths, molecular volume, flexibility of functional groups, but foremost the polarization of bonds because the umpolung principle is utilized,[10] see partial charges in Figure 1. Therefore, high-quality and high-

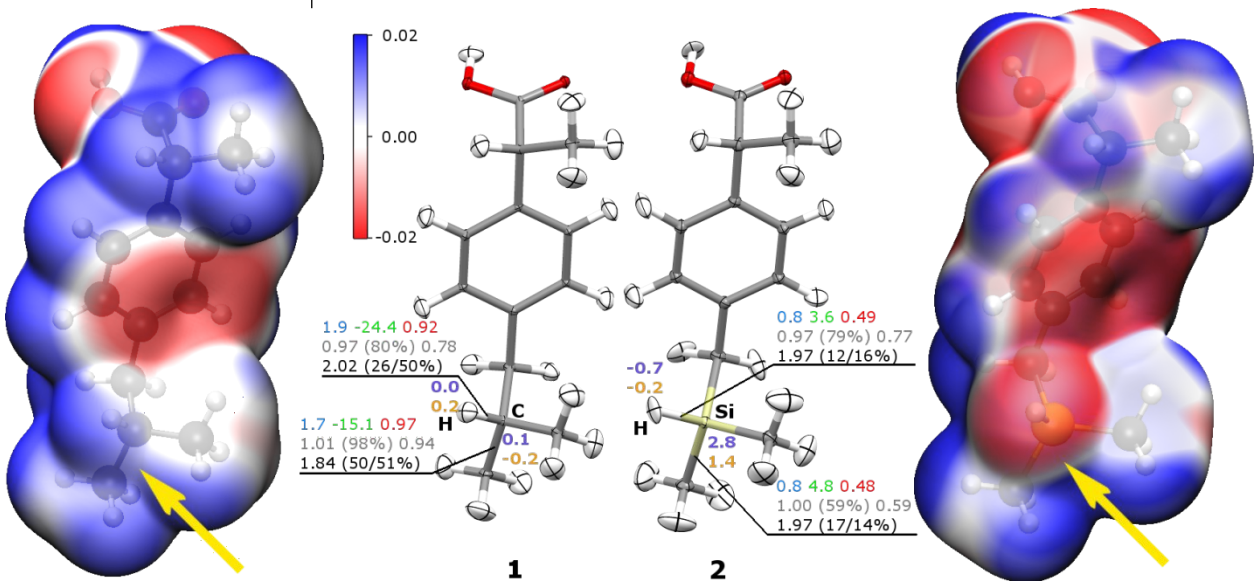

Figure 1. Electrostatic potential (in *e Å*$^{-1}$) of ibuprofen (**1**,left) and sila-ibuprofen (**2**,right), color-mapped onto the 0.001 *a.u.* electron-density isosurface derived by XWR. The refined molecular structures are shown with anisotropic displacement parameters for all atoms including hydrogen atoms at a 50% probability level. XWR-derived bond descriptors and atomic charges of the regions of the molecules most affected by the umpolung are given using the following color code [references to the methods used are given in the supporting information]: Quantum Theory of Atoms in Molecules (QTAIM) charge in e (purple), natural population analysis charge in e (orange), electron density in *eÅ*$^{-3}$ (blue) and its Laplacian in *eÅ*$^{-5}$ (green) at the QTAIM bond critical points, delocalization index (red), natural bond orbital bond order (gray) with percentage of covalent resonance structure derived from natural resonance theory analysis and natural localized molecular orbital NLMO/NPA bond order, population of electron localizability indicator bond basin (black) with contribution from C/Si in terms of QTAIM atomic basin volume/electron density.

resolution synchrotron X-ray diffraction experiments were performed on crystals of racemic mixtures of **1** and **2** (Table S1). Both compounds are isomorphous and crystallize in the monoclinic space group $P2_1/c$. Hence, molecular and solid-state structures are sterically nearly identical; the molecular volumes, determined within the electron-density isosurfaces shown in Figure 1, vary by only 7%. X-ray wavefunction refinement (XWR) was chosen as the crystallographic refinement method since it results in reliable hydrogen atom positions based on X-ray data.[11] The tertiary H–**C/Si** bond length difference is 0.374 Å, while H–**C/Si**–C bond angles only change by 0.68°, averaged over three neighboring bonds.

Accurate hydrogen-atom parameters are crucial for the derivation of reliable electrostatic properties and intermolecular interaction energies.[12] It was shown before that, as a first approximation, the polarization through intermolecular interactions of the biologically active compound in its crystal structure is similar to that in the enzyme.[13] The significant effect of the umpolung on the charges of the hydrogen atom by the carbon-silicon switch [q(C–***H***)=0.0 to 0.2 *e*; q(Si–***H***)=–0.2 to –0.7 *e*, Figure 1] is reflected by the electrostatic potential (ESP) of both molecules, calculated from the experimentally constrained wavefunctions. **1** shows a positive ESP near the tertiary carbon atom of the *iso*butyl group, while the same area is negative around the silane hydrogen atom in **2** (Figure 1). The Politzer parameters[14] for these surfaces show a higher internal charge separation for **2** (average deviation from the mean surface potential Π=0.0263 eÅ^{-1}) compared to **1** (Π=0.0240 eÅ^{-1}), see Table S2.

Moreover, XWR models chemical features of bonding and interactions from the experimental X-ray structure factors. Hence, an experimental complementary bonding analysis is feasible.[15] Those regions which are not directly affected by the silicon-carbon switch, e.g. the carboxylic acid group, show very similar intramolecular bonding features and atomic charges, but the umpolung of the Si–H bond in comparison to the C–H bond is reflected clearly by the descriptors in the direct vicinity (Figure 1, Data S3). The average electron density of the C/Si atoms and their immediate environment is a parameter complementary to the ESP and the bonding analysis. Whereas the latter reflect the polarization and govern the physical properties, the average electron density should be similar for a bioisosteric replacement.[16] Here, the values are indeed similar [0.047 a.u. (ibuprofen **1**) and 0.051 a.u. (sila-ibuprofen **2**)] for the C/Si atom plus the directly bonded methyl/methylene groups, but not as similar as for the bioisosteric tetrazole/carboxylate pair in ref. 16.

In an effort to understand the effect introduced by the differences in atomic and bonding properties for the molecular recognition and the mode of action, MD simulations and subsequent quantum-chemical results averaged over the entire MD trajectory were analyzed. For this purpose, we developed new methodology and related software (see supporting information). The available crystal structure of the complex of murine (COX-II) and **1** was taken from the protein crystallographic database (PDB code 4PH9)[17] and equilibrated in a solvation box with physiological sodium chloride solution. An identical procedure was applied upon substitution of **1**

residue	Ibuprofen (***1***) <$E_{disp/ele}$> (*kJ mol^{-1}*)	Sila-ibuprofen (***2***) <$E_{disp/ele}$> (*kJ mol^{-1}*)	wRMSD <E_{Sila}>-<E_{Ibu}>(*disp/ele*)
Arg	□17(1)/ □490(24)	□16(1)/ □490(30)	0.60/0.01
GlyAla	□41(6)/□28(4)	□35(5)/□22(4)	0.30/0.41
MetVal	□15(3)/2(4)	□21(4)/2(3)	0.49/0.07
Phe	□9(2)/1(1)	□14(4)/ □3(2)	0.49/0.76
SerLeu	□18(4)/ □20(2)	□22(5)/□27(4)	0.30/0.52
Tyr	□13(3)/ □9(5)	□11(3)/□19(7)	0.33/0.39
Σ	□113/□541	□119/□566	Δ=6/25

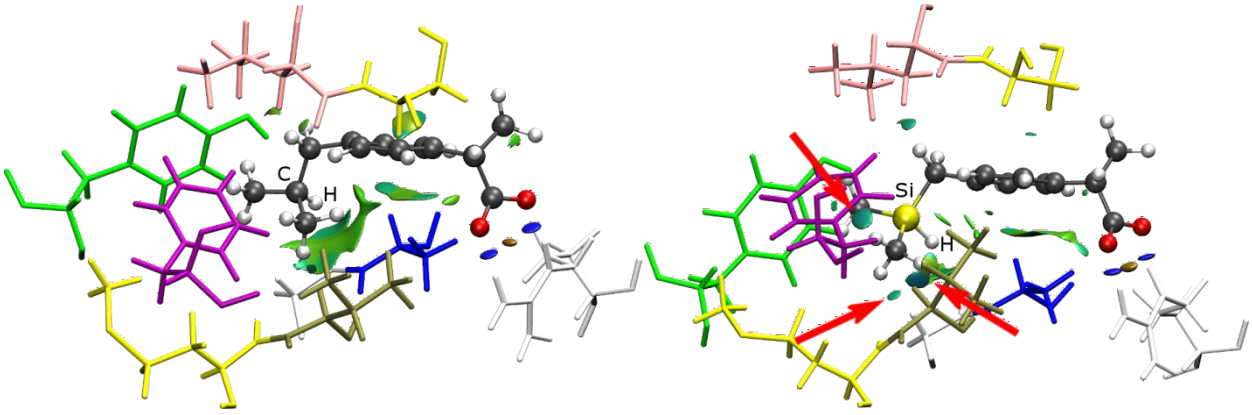

Figure 2. Visualization of residues important for close interactions inside the active site of COX-II after MD of ibuprofen (**1**,left) and sila-ibuprofen (**2**,right) (color code in the first column of the table). Visualization of the aNCI, color code: green = weak dispersion interactions, blue = stronger electrostatic interactions, orange = repulsive interactions. The table lists the corresponding pairwise interaction energies between the (sila)ibuprofen molecule and the amino-acid residues, separated into dispersion and electrostatic terms,[20] but here averaged over the entire trajectory of the MD simulation. Sample standard deviations are given in brackets, and weighted root-mean-square differences in a separate column. The authors refer to the supporting information for a full table of energies and a movie of the intermolecular interactions in the enzyme pocket.

by **2**. Missing force-field parameters involving the silicon atom were derived in the course of this work partially based on the XWR wavefunctions (Figures S12-S14, Tables S3-S5). Ibuprofen (**1**) and sila-ibuprofen (**2**) bonded to the active site of COX-II are shown in Figure 2 with closest residues of the protein explicitly visualized. Green and blue surfaces show the non-covalent interaction (NCI) index[18] averaged over 1000 different geometries throughout the production phase of the MD (aNCI).[19] It shows type and strength of all thermally stable contacts (Figure 2). In addition, thermally averaged pairwise intermolecular interaction energies are given in Figure 2.

The carboxylic acid group is the key motif for the recognition of **1** in COX-II,[3] which is reflected in Figure 2 by a large electrostatic interaction energy term with the Arg residue and by localized blue NCI surfaces. We find that the same is true for **2**, so thermal stability in the enzyme pocket is guaranteed (see also distance plot Figures S15-S16). Interactions of the phenyl ring of both **1** and **2** with the Gly-Ala residue as well as, surprisingly, the interactions involving the C-H and Si-H groups themselves are not favorably stabilizing **2** compared to **1**. Instead, the interactions of the two methyl and the methylene groups adjacent to the silicon atom are decisive for a total stabilization of **2** relative to **1** by about 10 kJ mol^{-1}, which includes the repulsion and polarization terms shown in Table S6 (Figures S18-S21).[20] The corresponding NCI regions (light blue-colored discs) representing the interactions of the methyl and methylene groups of sila-ibuprofen with the Met-Val, Phe and Ser-Leu residues are highlighted with arrows in Figure 2. A similar calculation for **1** *vs.* **2** binding to COX-I yields a stabilization of **1** by 19 kJ mol^{-1} (Figures S17,22-25 and Table S7). Both energy differences for binding to COX-I/II (10-20 kJ mol^{-1}) are small when compared to the total binding energies of around 760-770 kJ mol^{-1} (Tables S6 and S7), indicating similar activity of **1** and **2** against both enzymes, as confirmed by the IC_{50} values in Table 1.

In Free Energy Perturbation (FEP) calculations, a difference of the Gibbs free energy of 1.46 ± 0.14/–4.7 ± 0.2 kJ mol^{-1} was obtained when morphing ibuprofen (**1**) into sila-ibuprofen (**2**) inside COX-I/COX-II (Figures S26-S27).[21] This confirms again that **2** is bound to COX-I and -II approximately as strongly as ibuprofen **1**, however, both theoretical approaches (FEP and averaged interaction energies, previous paragraph) show a very small stabilization of sila-ibuprofen (**2**) in COX-II, but a small destabilization in COX-I. In a simplified model, inhibition of COX-II is responsible for pain relief, whereas inhibition of COX-I is responsible for side effects. This is promising because, in conjunction with the simple synthesis and improved solubility, it renders sila-ibuprofen (**2**) a potent candidate for drug development with the aim of obtaining a non-steroidal anti-inflammatory anti-rheumatic drug similarly potent as the gold-standard ibuprofen itself, but with improved properties for administering the drug.

Low toxicity is a prerequisite for any pharmaceutical application. To test for potential adverse effects of sila-ibuprofen (**2**) in comparison to ibuprofen (**1**) on mammalian cells, we have used C6 glioma cells, which are widely established as model systems to study functions and properties of brain glial cells and brain glioma.[22] The cells were exposed to **1** or **2** in concentrations of up to 1000 µM for up to 3 days. Application of 300 µM of either compound did not affect the proliferation of the cells. Furthermore, the viability of the cells was not affected by a 72 h exposure to up to 300 µM of **1** or **2** (Figure S28). These data confirm the low toxicity of ibuprofen (**1**),[3,23] and demonstrate also a low toxic potential of sila-ibuprofen (**2**) as no differences in the parameters determined were observed (Figure S28). In addition, the exposure of C6 cells to 1000 µM of **1** or **2** did not lead to any obvious change in cell morphology nor to any significant increase in extracellular lactate dehydrogenase activity, demonstrating that these high concentrations were not toxic to the cells either. Serum concentrations of ibuprofen in treated patients are in the low micromolar range,[24] suggesting that in situations for *in-vivo* application no toxicity is to be expected.

CONCLUSIONS AND OUTLOOK

Sila-ibuprofen has similar binding characteristics and a similar inhibitory profile towards COX-I and COX-II as ibuprofen, the gold-standard used for pain relief, but a higher solubility. This means that the carbon-silicon exchange acts as a bioisosteric replacement in the case of ibuprofen, but produces beneficial physical properties.

Further studies on the ability of sila-ibuprofen to act *in vivo* as inhibitor of COX activity as well as studies on the pharmacokinetics and pharmacodynamics of sila-ibuprofen *in vivo* are now highly desired to evaluate the pharmacological potential of sila-ibuprofen.

EXPERIMENTAL AND COMPUTATIONAL SECTION

Equipment, materials and methods

NMR spectra were recorded at room temperature on a Bruker Avance 600 spectrometer. ^{1}H, $^{13}C\{^{1}H\}$ and $^{29}Si\{^{1}H\}$ NMR spectra are reported on the δ scale (ppm) and are referenced against $SiMe_4$. ^{1}H and $^{13}C\{^{1}H\}$ chemical shifts are reported relative to the residual peak of the solvent ($(CD)_3(CD_2H)CO$ 2.09 ppm for $(CD_3)_2CO$) in the ^{1}H NMR spectra, and to the peak of the deuterated solvent ($(CD_3)_2CO$ 30.60 ppm) in the $^{13}C\{^{1}H\}$ NMR spectra.

The ESI (HR) MS spectra were measured on a Bruker Impact II spectrometer. Acetonitrile or dichloromethane/acetonitrile solutions ($c = 1 \cdot 10^{-5}$ *mol* L^{-1}) were injected directly into the spectrometer at a flow rate of 3 *µL* min^{-1}. Nitrogen was used both as a drying gas and for nebulization with flow rates of approximately 5 *L* min^{-1} and a pressure of 5 *psi*. Pressure in the mass analyzer region was usually about $1 \cdot 10^{-5}$ *mbar*. Spectra were collected for 1 *min* and averaged. The nozzle-skimmer voltage was adjusted individually for each measurement.

Electronic Impact Mass (EI MS) spectra were measured on a MAT 711 spectrometer, Varian MAT. Electron Energy for EI was set to 70 eV eV.

The microanalysis was obtained from a Vario EL elemental analyzer.

IR spectra were recorded with a Thermo Scientific Nicolet iS10 instrument.

Synthesis of 2-[(4-dimethylsilylmethyl)phenyl]propionic acid (**2**)[25]

In a schlenk flask under argon atmosphere, 2-[(4-bromomethyl)phenyl]propionic acid (1.00 *g*, 4.11 *mmol*) was dissolved in diethylether (25 *mL*) and stirred at room

temperature. Dimethylchlorosilane (1.56 *g*, 16.4 *mmol*) was added and triethylamine (0.832 *g*, 8.22 *mmol*) was added dropwise over the course of 5 minutes under the formation of a cloudy white solid. The reaction mixture was stirred for 24 hours and the solid was filtered and washed with dry diethylether (30 *mL*). A 3-neck round-bottom flask was equipped with a dropping funnel and a reflux condenser and charged with (*0.200 g, 8.22 mmol*) magnesium turnings. Under an argon atmosphere, the remaining solution was added dropwise to the magnesium turnings to obtain a constant reflux. Afterwards, the suspension was refluxed for additional 10 *h*. Under rapid stirring, ice water (50 *mL*) was added and the organic phase was separated and worked up aqueously with distilled water (3 × 25 *mL*). The solvent was removed under reduced pressure to yield a sticky oil which was purified by column chromatography by first flushing with 3 column volumes of *n*-hexane and subsequently eluting the product with ethyl acetate to give **2** as microcrystalline colorless solid (0.777 *g*, 85 % yield) after removal of the solvent.

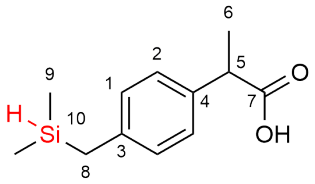

2

^{1}H NMR (acetone-d_6, 600 MHz) δ = 7.20 (d, $^{3}J(^{1}H\text{-}^{1}H)$= *8.1 Hz,* 2H; H-1,), 7.03 (d, $^{3}J(^{1}H\text{-}^{1}H)$= *8.1 Hz,* 2H; H-2), 3.91-3.95 (sept), $^{1}J(^{1}H\text{-}^{29}Si)$=*185 Hz,* $^{3}J(^{1}H\text{-}^{1}H)$=*3.5 Hz*, 1H; H-10), 3.68 (quart, $^{3}J(^{1}H\text{-}^{1}H)$= *7.2 Hz*, 1H; H-5), 2.16 (d, $^{3}J(^{1}H\text{-}^{1}H)$= *3.5 Hz*, 2 H; H-8), 1.40 (d, $^{3}J(^{1}H\text{-}^{1}H)$= *7.2 Hz,* 3 H; H-6), 0.05 (d, $^{3}J(^{1}H\text{-}^{1}H)$= *3.7 Hz,* 6 H; H-9) *ppm*.
^{13}C{^{1}H} NMR (acetone-d_6, 151 MHz) δ = 175.8 (C-7), 139.4 (C_{quart}), 138.0(C_{quart}), 129.0 ($C_{arom,}$ C-1), 128.2($C_{arom,}$ C-2), 45.2 (C-5), 23.9 (C-8), 19.1 (C-6), -4.7 (C-9) *ppm*.
^{29}Si{^{1}H} NMR (acetone-d_6, 119 MHz) δ = −11.5 *ppm*.
IR ν(Si-H): 2132 cm^{-1} (KBr-pallet).
UV λ_{max} (CH_2Cl_2): 234 *nm*.
Microanalysis Calc. for $C_{12}H_{18}O_2Si$ (222.36) C, 64.82; H, 8.16; Found C, 64.54; H, 8.55.
EI-MS (70 eV) (*m/z*): 222.4 $[M]^+$, calculated ($C_{12}H_{18}O_2Si$) = 222.1 *g/mol*
HR-ESI-MS (*m/z*):
$[M\text{-}H]^+$ calculated for $C_{12}H_{17}O_2Si$, 221.09923; found: 221.09926.
$[M\text{-}H]^-$ calculated for $C_{12}H_{17}O_2Si$, 221.10033; found: 221.10017.

Metabolites of **1** and **2**

Previous investigation into the metabolism of **1** exposed that it has two main metabolites that have been isolated in the urine of human subjects.[3] Characterization of these by infrared and nuclear magnetic resonance spectroscopies revealed that one of them is hydroxy-ibuprofen and that the other one is the corresponding carboxylic acid. [3]

Similarly, we assume that the oxidation of **2** in the liver should produce its respective silanol derivate.[9] In this context, we have synthesized hydroxy-sila-ibuprofen (**3**), through oxidation of compound **2** in the presence of a palladium catalyst using water as oxidation agent. Hydroxy-sila-ibuprofen (**3**) was prepared in acidic conditions, besides its condensation product, the disiloxane **4**. Both compounds are in an equilibrium with each other.

Synthesis and characterization of 2-(4-(hydroxydimethylsilyl-methyl)phenyl) propionic acid (**3**)

2 (500 *mg*, 2.25 *mmol*) dissolved in acetone (10.0 *mL*) was added to an ice cooled suspension of Pearlman's catalyst, $Pd(OH)_2/C$ (12.0 *mg*), in acetone (10.0 *mL*) and water (0.10 *mL*). After the evolution of hydrogen ceased, the reaction mixture was stirred at room temperature for 10 *min*. The reaction mixture was filtered to remove the catalyst and the solvent was removed from the remaining filtrate at 30 *°C* under reduced pressure. Removal of volatiles under reduced pressure afforded 480 *mg* (2.01 *mmol*, 89% yield) of the silanol **3** as a colorless oil.

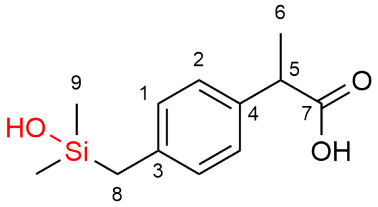

3

^{1}H NMR (acetone-d_6, 600 MHz) δ = 7.16 (d, $^{3}J(^{1}H\text{-}^{1}H)$ = *8.2 Hz*, 2H; H-1), 7.05 (d, $^{3}J(^{1}H\text{-}^{1}H)$ = *8.2 Hz*, 2H; H-2), 3.68 (quart, $^{3}J(^{1}H\text{-}^{1}H)$ = *7.1 Hz*, 1H; H-5), 2.11 (s, 2H; H-8), 1.41 (d, $^{3}J(^{1}H\text{-}^{1}H)$ = *7.1 Hz*, 2H; H 6), 0.04 (s, 6H; H-9) *ppm*.
^{13}C{^{1}H} NMR (acetone-d_6 151 MHz) δ = 175.7 (C-7), 138.7 (C_{quart}), 137.0 (C_{quart}), 128.7 (C-1), 127.5 (C-2), 44.8 (C-5), 27.8 (C-8), 18.6 (C-6), -0.94 (C-9) *ppm*.
^{29}Si{^{1}H} NMR (acetone-d_6, 119 MHz) δ = 14.5 *ppm*.
EI-MS (70 eV) (*m/z*): 238.0 $[M]^+$, calculated ($C_{12}H_{18}O_3Si$) = 238.1 *g/mol*.

Synthesis and characterization of the condensation product of **3**, the disiloxane **4**

3 (300 *mg*, 1.10 *mmol*) in acetone (100 *mL*) was diluted with water (12 *mL*) and concentrated HCl (2.50 *µL*) was added. The solution was left standing for 3 weeks. After this time, the volatiles were removed under reduced pressure to obtain 470 *mg* (1.02 *mmol*, 93% yield) of the disiloxane **4** as a colorless oil.

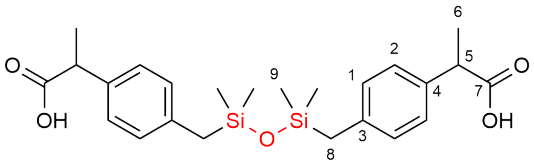

4

^{1}H NMR (acetone-d_6, 600 MHz) δ = 7.19 (d, $^{3}J(^{1}H\text{-}^{1}H)$ = *8.2 Hz*, H-1), 6.99 (d, $^{3}J(^{1}H\text{-}^{1}H)$ = *8.2 Hz*, 2H; H-2), 3.69 (quart, $^{3}J(^{1}H\text{-}^{1}H)$ = *7.1 Hz*, 1H; H-5), 2.08 (s, 2H; H-8), 1.42 (d, $^{3}J(^{1}H\text{-}^{1}H)$ = *7.1 Hz*, 2H; H-6), -0.01 (s, 6H; H-9) *ppm*.
^{13}C{^{1}H} NMR (acetone-d_6, 151 MHz) δ = 175.8 (C-7), 138.2 (C_{quart}), 137.1 (C_{quart}), 128.7 (C-1), 127.4 (C-2), 44.7 (C-5), 27.8 (C-8), 18.6 (C-6), -0.45 (C-9) *ppm*.
^{29}Si{^{1}H} NMR (acetone-d_6, 119 MHz) δ = 4.93 *ppm*.
ESI-MS: m/z = 481.2 $[M+Na]^+$, calculated ($C_{24}H_{34}O_5Si_2$+Na) = 481.6 *g/mol.*

Purity of the compounds

Purity of all compounds is > 95% as determined by HPLC and NMR spectroscopy.

In detail, ibuprofen **1** was obtained commercially with a purity ≥ 98%. Purity of sila-ibuprofen **2** is > 95% as determined by NMR and HPLC. Compounds **3** and **4** were investigated as metabolites and decomposition products of **2**. They are in equilibrium with each other and were not purified hence their biochemical properties are not subject of this paper.

Determination of the melting enthalpy

The melting enthalpy was determined using differential scanning calorimetry (DSC) of a sample of **1** and **2** using a Mettler-Toledo DSC3+ instrument with 40 μL aluminium crucibles with a pin (Mettler Toledo) and a pierced lid, referenced against an empty crucible with a pierced lid. The temperature program for the samples of **1** involved heating from 25 $°C$ to 125 $°C$ at 10 $K\ min^{-1}$ under a flow of N_2 at 20 $mL\ min^{-1}$. The temperature program for the samples of **2** involved heating from 0 $°C$ to 70 $°C$ at 10 $K\ min^{-1}$ under a flow of N_2 at 20 $mL\ min^{-1}$. Data evaluation was performed using the Software Star-e Version 15.01.

Solubility Determination

Solubility was determined in a HPLC/UV experiment, using an isocratic method with 1:1 ratio of water and acetonitrile with 0.1 $mol\ L^{-1}$ acetic acid as eluent on a RP-18 gravity column detecting the absorption at 235 nm, in agreement with the UV/VIS spectrum of **2**. **1** was used as an internal standard in a concentration of 0.1 $mg\ L^{-1}$, while equidistant calibration was done for **2** in steps of 5 $mg\ L^{-1}$ starting from 5 $mg\ L^{-1}$ until 55 $mg\ L^{-1}$. The resulting calibration plot is shown in Figure S1.

Determination of the stability of sila-ibuprofen (**2**) in solution

To investigate whether **2** is stable over time in physiological media, a solution of NaCl (0.9%) in water was used to dissolve **2**, until the solution was saturated in **2**. The solution was then kept at room temperature in an NMR tube and measured every 7 days. Additionally, an identical solution was prepared and kept at 4°C and measured every 28 days. Resulting spectra can be seen in Figures S5 and S6. These experiments show that, at room temperature, the solution slowly decomposes to the disiloxane **4** over the course of a month. At 4°C, decomposition is much slower, it only starts after the first month. Furthermore, the stability of **2** in physiological basic conditions (pH = 8) was tested as well. A solution of $NaHCO_3$ (10 mM) in D_2O was used to dissolve sila-ibuprofen **2**. Over the course of one month, no decomposition by ^{1}H-NMR was visible. Above a pH of 8 (tested at pH = 10 and 12), sila-ibuprofen decomposes under release of hydrogen to form the sodium salt of hydroxy-sila-ibuprofen **3.**

To complement the NMR experiments, the stability of **2** was tested on a high-performance liquid chromatography (HPLC) column under mildly acidic conditions. Purified sila-ibuprofen **2** was added onto the column, and only a single compound peak was observed after several minutes on the column for 14 repetitions of the experiment.

Crystallographic information

Single-crystals of **1** were obtained by slow evaporation of a saturated methanol solution in an open vessel. Crystals of **2** were obtained after chromatographic purification on silica gel, followed by removal of the solvent by low pressure evaporation and slow resublimation of **2** in a closed vessel. Information on the synchrotron measurements and pertinent crystallographic information obtained from the refinement of the structures of **1** and **2** are shown in Table S1. Datasets were measured at SPring-8, beamline BL02B1, at 25 K using a large cylindrical image plate camera.

The first step in the performed X-ray Wavefunction Refinement (XWR) is Hirshfeld Atom Refinement (HAR).[11] HAR uses tailor-made aspherical atomic scattering factors from a stockholder partitioning of the calculated static electron density. Here, B3LYP/def2-TZVPP was used and a surrounding cluster of point charges and dipoles of 8 $Å$ radius around the central molecule to simulate the crystal field. Subsequently, X-ray constrained wavefunction fitting as the second step in XWR was performed at RHF/def2-TZVPP without cluster charges to extract as much information as possible from the experimental structure factors. The program Tonto was used for the XWR procedure. From these wavefunctions, a 0.001 *a.u.* isosurface was calculated and the electrostatic potential mapped onto it, resulting in the Politzer parameters given in Table S2.

Force-field development and molecular dynamics simulations

To understand the active mode of sila-ibuprofen (**2**) in contrast to the one of conventional ibuprofen (**1**) on an atomistic scale, it was necessary to perform molecular dynamics (MD) simulations. Since the parameters for a CHARMM-type force field of **2** are unknown, they had to be derived by comparing energies obtained from ab-initio calculations with energies derived by the newly constructed force field. The unknown parameters of the force field are shown in Figure S12.

This procedure was carried out on the geometry and with the wavefunction obtained from XWR. Interaction energies with water for charge determination were calculated on a level of theory of HF/def2-TZVP, the bonded interactions were calculated on a level of theory of B3LYP/def2-TZVPP and the torsion potential energy surface scan was performed on a level of theory of MP2/def2-SVPP. The performance of the derived force field parameters in comparison to ab-initio calculations is visualized in Figure S13, showing the dihedral potential energy surface scan energies from reference calculations and energies calculated from the force field, both normalized to their smallest value.

Additionally, the energies of three rigid potential energy surface scans of two trimethyl silane molecules, used as a smaller model compound for the silane group in **2**, in orientations showing H-Si…H-Si, H-Si…Si-H and Si-H…H-Si contacts, were used to iteratively modify the parameters for the non-bonded interaction of the hydrogen atom of the silane group and the silicon atom itself to resemble observed energy profiles obtained on a level of theory of B3LYP-GD3BJ/def2-TZVP. The plots of these profiles can be seen in Figure S14. To validate these parameters in biological context, the active site of COX-II was taken from an equilibrated structure obtained using these parameters and the amino acids near **2** were then scanned in a radial elongation of the distance between amino acid and **2**. The obtained bonded parameters of the force field are shown in Table S3. The parameters for the Lennard Jones potential are shown in Table S4, charges assigned to the individual types of atoms in both **1** and **2** can be seen in Table S5.

The MD simulations and all derived properties (Supporting Information chapters 4-6) are based on available crystal structures of ibuprofen bonded to the active sites of COX-I and COX-II. Unfortunately, crystal structures of ibuprofen with human COX do not exist, so we had to resort to crystal structures of complexes of ibuprofen with ovine COX-I (PDB code 1EQG)[26] and murine COX-II (PDB code 4PH9).[17] Human and animal COX are pharmacologically not identical,[27] but they are by far the best models available for our study.

The derived force field parameters were used in addition to the parameters obtained for **1** from the swissparam service,[28] to describe ibuprofen (**1**) and sila-ibuprofen (**2**), while a CHARMM force field[29] was applied for the protein, sugars and heme residues, to perform MD for 400 *ns* on each complex inside a 110×110×110 $Å^3$ box including explicit water molecules (TIP3P) and sodium chloride ions corresponding to a concentration of 0.15 $mol\ L^{-1}$ using *NAMD2*.[30] The timestep chosen for the simulations was 1 *fs,* at a temperature of 300 *K* and a pressure of 1 *atm* used for prior equilibration. Periodic boundary conditions were used. After the equilibration, the system was simulated without thermostat or barostat to ensure that no outer influence caused changes in the binding of the drug molecule or conformational changes of the protein. A plot of the distance of both oxygen atoms of the carboxylic acid group to the corresponding arginine hydrogen bond donors is shown in Figures S15-S16.

Averaged non-covalent interaction index (aNCI)

The general idea of the *aNCI* was introduced by *Wu et al.*[19] who made their source code available. Since this approach needs many different evaluations of the NCI for the different geometries of the MD, the computational cost of this procedure is very high. For a system with a size of proteins and for long runs, this becomes too demanding to be done in a reasonable time scale. *Rubez et al.* wrote a kernel which performs the calculation of promolecular NCI calculations highly parallelized on graphics cards (*cuNCI*).[31] This source code is also available. Since during MD no wavefunction is available, only promolecular calculations are possible and therefore this kernel was optimal, so in this work we extended the general functionality of the graphics cards code by employing the averaging proposed by *Wu et al.*[19] The resulting program plugin is called acuNCI in reference to both previous programs. The gradient and electron density are calculated numerically on a grid and averaged after each volumetric dataset if finished. In principle, this approach would also be possible for wavefunction based calculations and could be done using a similar kernel, using wavefunctions obtained by QM/MM calculations. The program will be available free of charge, including also wavefunction based calculated property files, where calculation of numerical volumetric data is performed on graphics cards. The results of these calculations are shown in a video, moving the viewer through the protein and binding pocket of COX-II in 3D in Movie S1.

Averaged interaction energies

To quantify the differences in interaction between amino-acid-residues and sila-ibuprofen (**2**) in contrast to ibuprofen (**1**), the simulations for the aNCI plots were used to calculate the interaction energies, using the program *tonto* (commit 5ba65f7 on github, https://github.com/dylan-jayatilaka/tonto) which is the backend of *CrystalExplorer*,[32] known for calculations of interaction energies and energy frameworks.[20,33] Since amino acids in proteins are part of a bigger molecule, it was necessary to saturate the bonds with hydrogen atoms that were cut when extracting individual residue coordinates from the protein. Hydrogen atoms were added using internal z-matrix notation for the determination of the positions, using a bond length of 1.07 *Å* for hydrogen atoms bonded to the N-terminus and 1.00 *Å* for the C-terminal hydrogen atoms. sp^2-hybridisation of the corresponding atom was assumed, using an ideal angle of 120° for the H-N/C-C_α angle and 180° for the dihedral angle using the carboxy-oxygen. A script to automatically calculate wavefunctions on a level of theory of B3LYP/6-31G(d,p) for the resulting amino acids was used, to calculate wavefunctions for 1,000 different frames of all 13 amino acids, each 1 *ps* apart during the MD for both simulations in COX-II and 12 residues with identical timing for COX-I. Each wavefunction was then analyzed using *tonto* and the four terms of the interaction energy, as well as total energy, plotted in Figures S18 – S21 for COX-II and S22 – S25 for COX-I. The averaged values, as well as standard uncertainties, are shown in Tables S6 and S7, respectively. The residues which had the closest distance around the silicon function and were used to define the energy difference given in the results section (Figure 2) are highlighted by color in these tables.

Free energy perturbation (FEP) calculations

Using the Free Energy Perturbation method[21] in *NAMD2*[30] using ParseFEP[34], the calculation of a so called "alchemical" transformation is possible, which describes in this case the gradual exchange of the C atom in ibuprofen by Si, and the parameters associated with this, as well as the neighboring atoms, as affected by the change of the force field. In principle, there are always both atoms present in the calculation, while their contribution to the system is weighted by the multiplicator λ, which is changed throughout the simulation from 0.0 to 1.0, in an interval size of 0.025 with 100,000 timesteps for equilibration of the system prior to evaluation of the FEP density of states, as well as energetics during 500,000 timesteps following, before increasing the λ interval, once more. Resulting plots for forward ($\lambda \in [0.0,1.0]$) and backwards ($\lambda \in [1.0,0.0]$) transformation of density of states and convergence of energy in the system are plotted in Figures S26-S27.

Cell toxicological investigation

To test for potential adverse effects of **1** or **2** on mammalian cells, we have used C6 glioma cells, a cell which is widely used as model system to study functions and properties of brain glial cells and brain glioma.[22,35] The cells were exposed to either **1** or **2** in concentrations of up to 1000 μM for up to 3 days. Application of 300 μM of these compounds did not affect the proliferation of the cells as demonstrated by the absence of any significant difference in the increase in cellular activity of the enzyme lactate dehydrogenase (LDH) compared to control cells (Fig. S24 A,B). Furthermore, the viability of the cells was not affected by a 72 *h* exposure to up to 300 μM **1** or **2** as indicated by the absence of any significant increase in extracellular LDH activity (Fig. S24 C), by the at best low loss in cellular protein per well (Fig. S24 D), by the unaltered WST1 reduction capacity (Fig. S24 E) and by an almost unaltered cellular lactate production (Fig. S24 F). These data confirm the low toxic potential of **1**,[3,24] and demonstrate also a

low toxic potential of **2** as no differences in the parameters determined were observed for cells that had been treated either **1** or **2** in concentrations of 100 μM or 300 μM (Fig. S24 A-F). Also, the exposure of C6 cells to 1000 μM of **1** or **2** did not lead to any obvious change in cell morphology (data not shown) nor to any significant increase in extracellular LDH, demonstrating that also these high concentrations were not toxic to the cells. However, in a concentration of 1000 μM both compounds drastically lowered cell proliferation (Fig. S24 A,B). Concerning this antiproliferative effect, 1000 μM **2** appeared to have a slightly higher potential as 1000 μM **1** as indicated by the significantly lower values determined for cellular LDH activity (Fig. S24 A,B), cellular protein content (Fig. S24 D) as well as cellular WST1 reduction capacity (Fig. S24 E). Nevertheless, it should be considered that the serum concentrations of **1** in treated patients are in the low micromolar range[24] suggesting that the antiproliferative effect observed for very high concentrations of **1** or **2** will not be relevant for an *in vivo* situation. A potential reason for the antiproliferative action of **1** applied in high concentrations may be its reported side-effect to uncouple the mitochondrial respiratory chain[36] which will diminish mitochondrial ATP production and thereby slow down cell proliferation.

Enzyme activity measurements to determine IC_{50} values

Inhibition studies of COX-I and COX-II and determination of the IC_{50} of the enzymes by **1** and **2** were performed by the company Eurofins Cerep (Le Bois L'Êveque, France) according to ref. 37 using human recombinant COX-I and -II enzymes from Sf9 cells in buffered saline. The test substrates applied were 1.2 μM arachidonic acid and 25 μM ADHP and the incubation times were 3 *min* (COX-I) and 5 *min* (COX-II). The activity was measured by monitoring resorfurin content as a measure for activity quantified using fluorimetry. Concentrations were selected in half-logarithmic steps in a range from 0.1 μM up to 100 μM test substance. The resulting % inhibitions are given in Table S8, visualized in Figure S29 with two reference substances for each enzyme. Regression of the data was performed using a model of

$$Y = D + \left(\frac{A - D}{1 + \left(\frac{C}{IC_{50}} \right)^{n}} \right)$$

employing the commercial software SigmaPlot 4.0 and Hill software. (Y=Activity, A= left asymptote, D=right asymptote, C=Concentration, IC_{50}=Concentration of half-maximal inhibition and n=Hill coefficient).

ASSOCIATED CONTENT

Supporting Information

The Supporting Information is available free of charge at https://pubs.acs.org/doi/xxx.

Supporting Information PDF. This file contains details about characterization, quantum crystallography, force-field development, the averaged non-covalent interaction index (aNCI), the averaged interaction energies, free energy perturbation (FEP) calculations, toxicological investigations, enzyme activity measurements to determine IC_{50} values, references to methods and software used in the bonding analysis.

Movie S1. Guided visual representation of the sila-ibuprofen – COX-II complex with aNCI isosurfaces and a comparison to the aNCI of the ibuprofen – COX-II complex. (MP4 video file)

Data S1. Interaction energies for molecular dynamics simulations of COX-I and COX-II complexes. (Spreadsheet .xlsx file)

Data S2. Bond lengths of molecular dynamics simulations. (Spreadsheet .xlsx file)

Data S3. Bond properties of complementary bonding analyses. (Spreadsheet .xlsx file)

Data S4. CIFs of **1** and **2**, including structure factors and ceckCIF reports. (.cif and PDF)

Data S5. Names, SMILES notation and IC_{50} values of ibuprofen **1** and sila-ibuprofen **2**. (.csv file)

AUTHOR INFORMATION

Corresponding Authors

Prof. Dr. Jens Beckmann, j.beckmann@uni-bremen.de; PD Dr. Simon Grabowsky, simon.grabowsky@dcb.unibe.ch

Notes

The authors declare no competing financial interests.

ACKNOWLEDGMENTS

In memory of the late Professor Werner Reutter, Charité Berlin. Special thanks to Lucio Colombi Ciacchi and Steffen Lid for helpful discussions on the force field development. The synchrotron-radiation experiments were performed on the BL02B1 beamline of SPring-8 with the approval of the Japan Synchrotron Radiation Research Institute (JASRI) under proposal No. 2017A1233. Funded by: Studienstiftung des Deutschen Volkes (Promotionsstipendium); Deutsche Forschungsgemeinschaft: GR 4451/1-1, GR 4451/2-1 and BE 3716/7-1; Forschungskommision Freie Universität Berlin; Forschungskommision Universität Bremen (Brückenstipendium).

ABBREVIATIONS

XWR, X-ray wavefunction refinement; QTAIM, Quantum theory of atoms in molecules; NLMO, Natural localized molecular orbital; NPA, Natural population analysis; ESP, Electrostatic potential; NCI, Non-covalent interaction; aNCI, Averaged non-covalent interaction; FEP, Free energy perturbation; DSC, Differential scanning calorimetry; HAR, Hirshfeld atom refinement; LDH, Lactate dehydrogenase

REFERENCES

(1) 21st WHO Essential Medicines List (EML), World Health Organization, **2019**. www.who.int/medicines/publications/essentialmedicines (accessed August 6th, 2020).

(2) Prusakiewicz, J. J.; Duggan, K. C.; Rouzer, C. A.; Marnett, L. J. Differential sensitivity and mechanism of inhibition of COX-2

oxygenation of arachidonic acid and 2-arachidonoylglycerol by ibuprofen and mefenamic acid. *Biochemistry* **2009**, *48*, 7353-7355.
(3) Rainsford, K. D. Ibuprofen Discovery, Development and Therapeutics. Wiley-Blackwell, Hoboken, New Jersey, U.S.A., **2015**.
(4) (a) Franz, A.; Wilson, S. O. Organosilicon molecules with medicinal applications. *J. Med. Chem.* **2013**, *56*, 388-405. (b) Ramesh, R.; Reddy, D. S. Quest for novel chemical entities through incorporation of silicon in drug scaffolds. *J. Med. Chem.* **2018**, *61*, 3779-3798.
(5) Romero, A.; Rhodes, C. Stereochemical aspects of the molecular pharmaceutics of ibuprofen. *J. Pharm. Pharmacol.* **1993**, *45*, 258-262.
(6) Xu, F.; Sun, L.-X.; Tan, Z.-C.; Liang, J.-G.; Li, R.-L. Thermodynamic study of ibuprofen by adiabatic calorimetry and thermal analysis. *Thermochim. Acta.* **2004**, *412*, 33-57.
(7) Yalkowsky, S. H.; He, Y.; Jain, P. *Handbook of aqueous solubility data.* CRC press, Boca Raton, USA, **2016**.
(8) (a) Riendeau, D.; Charleson, S.; Cromlish, W.; Mancini, J. A.; Wong, E.; Guay, J. Comparison of the cyclooxygenase-1 inhibitory properties of nonsteroidal anti-inflammatory drugs (NSAIDs) and selective COX2-inhibitors, using sensitive microsomal and platelet assays. *Can. J. Physiol. Pharmacol.* **1997**, *75*, 1088-1095. (b) Riendeau, D.; Percival, M. D.; Brideau, C.; Charleson, S.; Dubé, D.; Ethier, D.; Falgueyret, J.-P.; Friesen, R. W.; Gordon, R.; Greig, G.; Guay, J.; Mancini, J.; Ouellet, M.; Wong, E.; Xu, L.; Boyce, S.; Visco, D.; Girard, Y.; Prasit, P.; Zamboni, R.; Rodger, I. W.; Gresser, M.; Ford-Hutchinson, A. W.; Young, R. N.; Chan, C.-C. Etoricoxib (MK-0663): Preclinical profile and comparison with other agents that selectively inhibit cyclooxygenase-2. *J. Pharmacol. Exp. Ther.* **2001**, *296*, 558-566. (c) Kato, M.; Nishida, S.; Kitasato, H.; Sakata, N.; Kawai, S. Cyclooxygenase-1 and cyclooxygenase-2 selectivity of non-steroidal anti-inflammatory drugs: investigation using human peripheral monocytes. *J. Pharm. Pharmacol.* **2001**, *53*, 1679-1685.
(9) (a) Kan, S. B. J.; Russel, R. D.; Chen, K.; Arnold, F. H. Directed evolution of cytochrome c for carbon-silicon bond formation: Bringing silicon to life. *Science* **2016**, *354*, 1048-1051. (b) Bähr, S.; Brinkmann-Chen, S.; Garcia-Borras, M.; Roberts, J. M.; Katasoulis, D. E.; Houk, K. N.; Arnold, F. H. Selective Enzymatic Oxidation of Silanes to Silanols. *Angew. Chem. Int. Ed*. **2020**, *59*, 15507-15511.
(10) Seebach, D. Methods of reactivity umpolung. *Angew. Chem. Int. Ed. Engl.* **1979**, *18*, 239-258.
(11) (a) Woińska, M.; Grabowsky, S.; Dominiak, P. M.; Woźniak, K.; Jayatilaka, D. Hydrogen atoms can be located accurately and precisely by x-ray crystallography. *Sci. Adv.* **2016**, *2*, e1600192. (b) Woińska, M.; Jayatilaka, D.; Dittrich, B.; Flaig, R.; Luger, P.; Woźniak, K.; Dominiak, P. M.; Grabowsky, S. Validation of x-ray wavefunction refinement. *Chem. Phys. Chem.* **2017**, *18*, 3334–3351.
(12) Müller-Dethlefs, K.; Hobza, P. Noncovalent interactions: A challenge for experiment and theory. *Chem. Rev.* **2000**, *100*, 143–167.
(13) Mladenovic, M.; Arnone, M.; Fink, R. F.; Engels, B. Environmental effects on charge densities of biologically active molecules: Do molecule crystal environments indeed approximate protein surroundings? *J. Phys. Chem. B* **2009**, *113*, 5072–5082.
(14) Politzer, P.; Murray, J. S.; Peralta-Inga, Z. Molecular surface electrostatic potentials in relation to noncovalent interactions in biological systems. *Int. J. Quantum Chem.* **2001**, *85*, 676–684.
(15) Fugel, M.; Malaspina, L. A.; Pal, R.; Thomas, S. P.; Shi, M. W.; Spackman, M. A.; Sugimoto, K.; Grabowsky, S. Revisiting a historic concept using experimental quantum crystallography: Are phosphate, sulfate and perchlorate anions hypervalent? *Chem. Eur. J.* **2019**, *25*, 6523–6532.
(16) Matta, C. F.; Arabi, A. A.; Weaver, D. F. The bioisosteric similarity of the tetrazole and carboxylate anions: Clues from the topologies of the electrostatic potential and of the electron density. *Eur. J. Med. Chem.* **2010**, *45*, 1868–1872.
(17) Orlando, B. J.; Lucido, M. J.; Malkowski, M. G. The structure of ibuprofen bound to cyclooxygenase-2. *J. Struct. Biol.* **2015**, *189*, 62-66.
(18) Johnson, E. R.; Keinan, S.; Mori-Sanchez, P.; Contreras-Garcia, J.; Cohen, A. J.; Yang, W. Revealing noncovalent interactions. *J. Am. Chem. Soc.* 2010, *132*, 6498-6506.
(19) Wu, P.; Chaudret, R.; Hu, X.; Yang, W. Noncovalent interaction analysis in fluctuating environments. *J. Chem. Theory Comput.* **2013**, *9*, 2226-2234.
(20) Turner, M. J.; Grabowsky, S.; Jayatilaka, D.; Spackman, M. A. Accurate and efficient model energies for exploring intermolecular interactions in molecular crystals. *J. Phys. Chem. Lett.* **2014**, *5*, 4249–4255.
(21) Dixit, S. B.; Chipot, C. Can absolute free energies of association be estimated from molecular mechanical simulations? The biotin–streptavidin system revisited. *J. Phys. Chem. A* **2001**, *105*, 9795–9799.
(22) Lenting, K.; Verhaak, R.; ter Laan, M.; Wesseling, P.; Leenders, W. Glioma: experimental models and reality. *Acta Neuropathol.* **2017**, *133*, 263-282.
(23) Berns, M.; Toennessen, M.; Koehne, P.; Altmann, R.; Obladen, M. Ibuprofen augments bilirubin toxicity in rat cortical neuronal culture. *Pediatr. Res.* **2009**, *65*, 392-396.
(24) Davies, N. M. Clinical pharmacokinetics of ibuprofen. *Clin. Pharmacokinet.* **1998**, *34*,101-154.
(25) Patent application by J. Beckmann, A. Justies: Silicon containing compounds and their use as anti-inflammatory agents From *PCT Int. Appl.* (2009), WO 2009004063 A1 20090108, and J. Beckmann, A. Justies: Silicon containing compounds and their use as anti-inflammatory agents From *Eur. Pat. Appl.* (**2009**), EP 2011502 A1 20090107.
(26) Selinsky, B. S.; Gupta, K.; Sharkey, C. T.; Loll, P. J. Structural analysis of NSAID binding by prostaglandin H2 synthase: time-dependent and time-independent inhibitors elicit identical enzyme conformations. *Biochemistry* **2001**, *40*, 5172-5180.
(27) Ramesha, C. S. "Human and rat cyclooxygenases are pharmacologically distinct" in *Eicosanoids and other bioactive lipids in cancer, inflammation, and radiation injury 3*. Springer, Boston, MA, **1997**, 67-71.
(28) Zoete, V.; Cuendet, M. A.; Grosdidier, A.; Michielin, O. SwissParam: a fast force field generation tool for small organic molecules. *J. Comput. Chem.* **2011**, *32*, 2359-2368.
(29) (a) MacKerell, A. D.; Feig, M.; Brooks, C. L. Extending the treatment of backbone energetics in protein force fields: Limitations of gas-phase quantum mechanics in reproducing protein conformational distributions in molecular dynamics simulations *J. Comput. Chem.* **2004**, *25*, 1400-1415. (b) MacKerell, A. D.; Bashford, D.; Bellott, M.; Dunbrack, R. L.; Evanseck, J. D.; Field, M. J.; Fischer, S.; Gao, J.; Guo, H.; Ha, S.; Joseph-McCarthy, D.; Kuchnir, L.; Kuczera, K.; Lau, F. T. K.; Mattos, C.; Michnick, S.; Ngo, T.; Ngyuen, D. T.; Prodhom, B.; Reiher, W. E.; Roux, B.; Schlenkrich, M.; Smith, J. C.; Stote, R.; Straub, J.; Watanabe, M.; Wiorkiewicz-Kuczera, J.; Yin, D.; Karplus, M. All-atom empirical potential for molecular modeling and dynamics studies of proteins. *J. Phys. Chem. B*, **1998**, *102*, 3586-3616.
(30) (a) Kalé, L.; Skeel, R.; Bhandarkar, M.; Brunner, R.; Gursoy, A.; Krawetz, N.; Phillips, J.; Shinozaki, A.; Varadarajan, K.; Schulten, K. NAMD2: greater scalability for parallel molecular dynamics. *J. Comput. Phys.* **1999**, *151*, 283-312. (b) Phillips, J.; Braun, R.; Wang, W.; Gumbart, J.; Tajkhorshid, E.; Villa, E.; Chipot, C.; Skeel, R. D.; Kalé, L.; Schulten, K. Scalable molecular dynamics with NAMD. *J. Comput. Chem.* **2005**, *26*, 1781-1802.
(31) Rubez, G.; Etancelin, J. M.; Vigouroux, X.; Krajecki, M.; Boisson, J. C.; Hénon, E. GPU accelerated implementation of NCI calculations using promolecular density. *J. Comput. Chem.* **2017**, *38*, 1071-1083.
(32) Turner, M. J.; McKinnon, J. J.; Wolff, S. K.; Grimwood, D. J.; Spackman, P. R.; Jayatilaka, D.; Spackman, M. A. *CrystalExplorer17* **2017**, University of Western Australia. (hirshfeldsurface.net)
(33) (a) Mackenzie, C. F.; Spackman, P. R.; Jayatilaka, D.; Spackman, M. A. CrystalExplorer model energies and energy frameworks: extension to metal coordination compounds, organic salts, solvates and open-shell systems. *IUCrJ* **2017**, *4*, 575-587. (b) Turner, M. J.; Thomas, S. P.; Shi, M. W.; Jayatilaka, D.; Spackman, M. A. Energy frameworks: insights into interaction anisotropy and the mechanical properties of molecular crystals. *Chem. Commun.* **2015**, *51*, 3735-3738.
(34) Liu, P.; Dehez, F.; Cai, W.; Chipot, C. A. A toolkit for the analysis of free-energy perturbation calculations. *J. Chem. Theor. Comput.* **2012**, *8*, 2606-2616.
(35) (a) Barth, R. F.; Kaur, B. Rat brain tumor models in experimental neuro-oncology: the C6, 9L, T9, RG2, F98, BT4C, RT-2 and CNS-1 gliomas. *J. Neuro.-Oncol.* **2009**, *94*, 299-312. (b) Grobben, B.; De Deyn, P. P.; Slegers, H. Rat C6 glioma as experimental model system for the

study of glioblastoma growth and invasion. *Cell Tissue Res.* **2002**, *310*, 257-270.

(36) Browne, G. S.; Nelson, C.; Nguyen, T.; Ellis, B. A.; Day, R. O.; Williams, K. M. Stereoselective and substrate-dependent inhibition of hepatic mitochondrial β- oxidation and oxidative phosphorylation by the non-steroidal anti-inflammatory drugs ibuprofen, flurbiprofen, and ketorolac. *Biochem. Pharmacol.* **1999**, *57*, 837-844.

(37) Vanachayangkul, P.; Tolleson, W. H. Inhibition of heme peroxidases by melamine. *Enzyme Research* **2012**, *416062*:1-7.

For Table of Contents Only